Report

Current Biology

Biogeography confounds the signal of cospeciation in Batesian mimicry

Graphical abstract

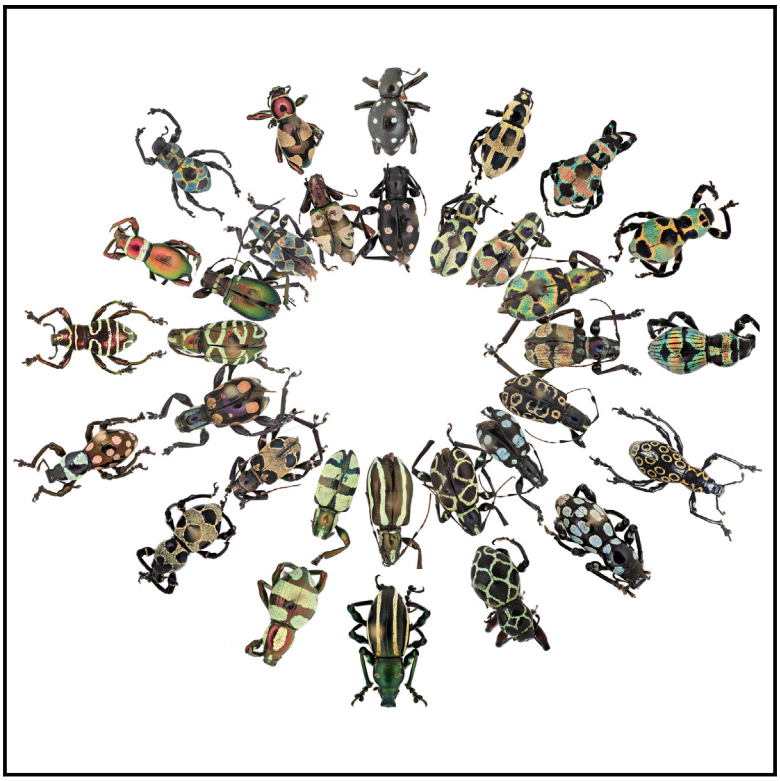

Highlights

- Coevolutionary interactions arise from community assembly events, not host tracking
- Structural colors in model and mimetic systems use different nano-level mechanisms
- We resolved the phylogeny of *Doliops* using a design of more than 30,000 UCE loci

Authors

Matthew H. Van Dam, Alessandro Parisotto, Milton N. Medina, Analyn A. Cabras, Nayeli Gutiérrez-Trejo, Bodo D. Wilts, Athena W. Lam

Correspondence

mvandam@calacademy.org (M.H.V.D.), bodo.wilts@plus.ac.at (B.D.W.)

In brief

To what extent are coevolutionary interactions conserved (i.e., lineage-constrained)? Are codiversification patterns primarily driven by biotic or abiotic factors? Van Dam et al. examine these questions using a beetle mimicry system and find that abiotic factors from their biogeographic history primarily influence their pattern of cospeciation.

Van Dam et al., 2024, Current Biology *34*, 5554–5563
December 2, 2024
https://doi.org/10.1016/j.cub.2024.09.084

CellPress

CellPress
OPEN ACCESS

Current Biology

Report

Biogeography confounds the signal of cospeciation in Batesian mimicry

Matthew H. Van Dam,[1,10,*] Alessandro Parisotto,[2,3] Milton N. Medina,[4,5] Analyn A. Cabras,[4,5] Nayeli Gutiérrez-Trejo,[6,7] Bodo D. Wilts,[3,8,*] and Athena W. Lam[9]

[1]Entomology Department, Institute for Biodiversity Science and Sustainability, California Academy of Sciences, San Francisco, CA, USA
[2]Adolphe Merkle Institute, University of Fribourg, Chemin des Verdiers 4, Fribourg, Switzerland
[3]Swiss National Center of Competence in Research Bio-Inspired Materials, University of Fribourg, Chemin des Verdiers 4, Fribourg, Switzerland
[4]Invertebrate Research Laboratory, UResCom, Davao Oriental State University, City of Mati 8200, Davao Oriental, Philippines
[5]Zoology Division, National Museum of Natural History, Malate, Manila, Philippines
[6]Division of Invertebrate Zoology, American Museum of Natural History, New York, NY, USA
[7]Richard Gilder Graduate School, American Museum of Natural History, New York, NY, USA
[8]Department of Chemistry and Physics of Materials, University of Salzburg, Jakob-Haringer-Str. 2a, Salzburg, Austria
[9]Center for Comparative Genomics, Institute for Biodiversity Science and Sustainability, California Academy of Sciences, San Francisco, CA, USA
[10]Lead contact
*Correspondence: mvandam@calacademy.org (M.H.V.D.), bodo.wilts@plus.ac.at (B.D.W.)
https://doi.org/10.1016/j.cub.2024.09.084

SUMMARY

Since the inception of the field of evolution, mimicry has yielded insights into foundational evolutionary processes, including adaptive peak shifts, speciation, and the emergence and maintenance of phenotypic polymorphisms.[1–3] In recent years, the coevolutionary processes generating mimicry have gained increasing attention from researchers. Despite significant advances in understanding Batesian and Müllerian mimicry in Lepidopteran systems, few other mimetic systems have received similar detailed research. Here, we present a Batesian mimicry complex involving flightless, armored *Pachyrhynchus* weevils and their winged *Doliops* longhorn beetle mimics and examine their coevolutionary patterns within the Philippine archipelagos. *Pachyrhynchus* weevils are primarily found in the Philippines, where distinct species radiations have occurred on different islands, each with unique color patterns serving as a warning to predators. This defensive trait and mimicry between unrelated species were first described by Wallace in 1889. Notably, the distantly related longhorn beetle *Doliops*, despite being soft-bodied and ostensibly palatable, mimics the heavily armored, flightless *Pachyrhynchus*. To address mimicry in this system, we reconstructed the phylogeny of *Doliops* using a probe set consisting of 38,000 ultraconserved elements. Our study examines the following questions central to understanding the *Pachyrhynchus-Doliops* mimicry system: (1) to what extent are coevolutionary interactions conserved (i.e., lineage-constrained) and (2) are the codiversification patterns primarily driven by biotic or abiotic factors?[4–6] To assess color mimicry and cospeciation, we examined the evolution of nanostructure-based warning colors and the effect of island biogeography on cospeciation. Our findings demonstrate the beetle's ability to repeatedly evolve multiple solutions to similar evolutionary challenges, evolving similar color patterns using different types of photonic crystals with varying degrees of order. We revealed that the observed pattern of cospeciation is driven mainly by abiotic factors from their biogeographic history. Unlike the patterns of coevolution seen between angiosperms and insect lineages,[7] most ecological interactions do not persist longer than a few million years, leading to patterns of modularity rather than ecological nestedness.[4,6,7]

RESULTS

To study the *Doliops-Pachyrhynchus* Batesian mimicry complex, we investigated the presence of conserved (lineage-constrained) coevolutionary interactions based on a phylogenomic analysis and traced the development of the mimicry complexes over time (Figures 1 and 2) to understand how conserved or labile they are. Second, we examined the patterns of cospeciation to determine the influence of abiotic factors by investigating the biogeography of species restricted to different Philippine islands. To accomplish this, we examined how biogeography affects these results by studying species restricted to different islands in the Philippines. Finally, we determined whether the nanostructure (ordered vs. disordered photonic crystals [PCs]) of the mimic corresponded to the nanostructure of the model species.

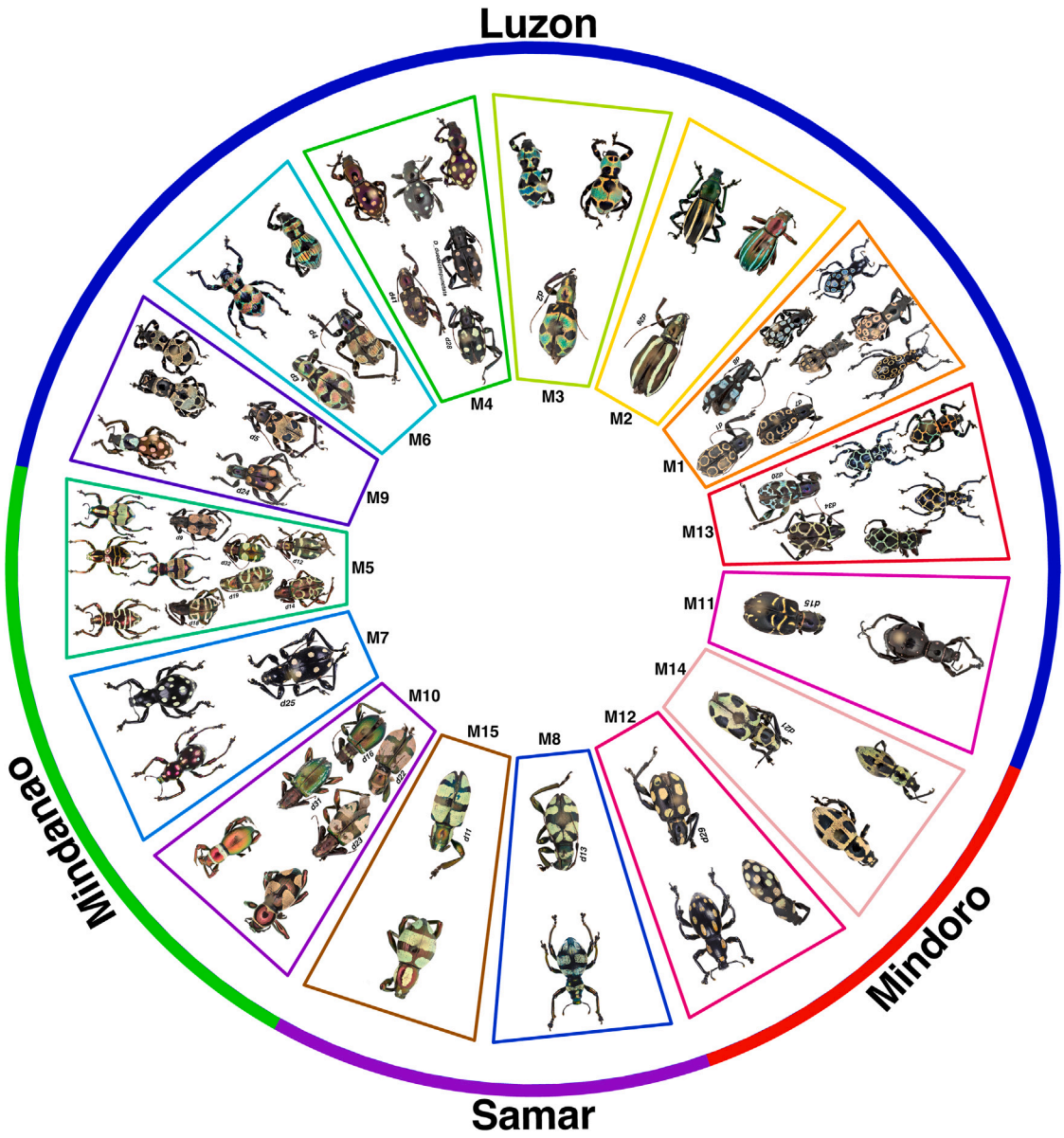

Figure 1. *Doliops-Pachyrhynchus* mimicry complexes

Trapezoids indicate modules identified by *evolnets* R package with >50% posterior probability threshold, module number at innermost center. Modules were derived from an ancestral host repertoire (or mimicry-rings) reconstruction analysis,[5] which assigns taxa to modules based on their interaction probabilities. *Pachyrhynchus* model species are toward the outer circle, and *Doliops* mimics are presented in the inner circle. The numbers to the left of the *Doliops* specimens are the voucher specimen codes. The outermost circle is colored by the island where the species occur.

Genomic assembly, phylogenomics, and biogeographic patterns of *Doliops*

Our genomic sequencing results returned, on average, 52,781,255 bp paired-end Illumina reads (95% highest density interval [HDI] 23,900,966–72,779,113 bp). The mean N50 length was 1,036 bp (HDI 429–1,999 bp), and the average number of BUSCO complete genes was 61.1% (HDI 31.9%–86.1%). The total assembly size averaged 603,435,064 bp (HDI 158,171,893–1,014,239,255 bp). After aligning probes to our genomes, we identified 38,173 ultraconserved element (UCE) loci, retaining 10,294 alignments after filtering (<80% complete, n = 35/44). The 80% complete matrices captured a mean and median of 8,461 and 9,701 loci per taxa, respectively. We combined cogenic UCEs, resulting in a total length of 8,219,151 bp.

We used the programs ASTRAL-MP and RAxML-NG to reconstruct the phylogeny of the mimic beetle taxon *Doliops*. Both produced similar trees, identifying the same main clades: a Luzon clade with a diffuse anterior band on the pronotum, a second clade in the Visayas, Mindoro, and Mindanao, and a third clade restricted to Mindanao (Figure 2). Differences between the trees did not result in any tip moving between main clades (see Figure S1). The RAxML tree had high support (>95 bs), except

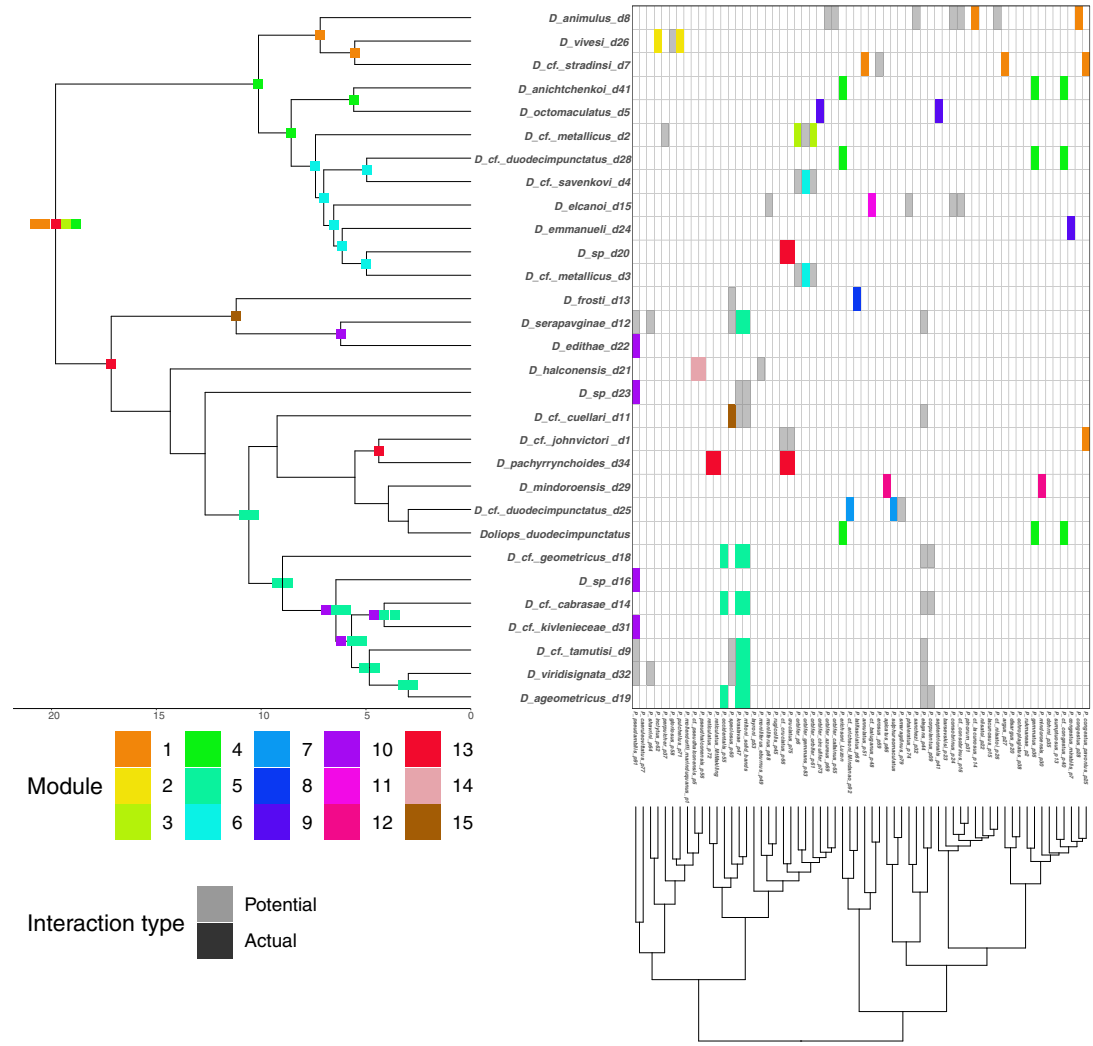

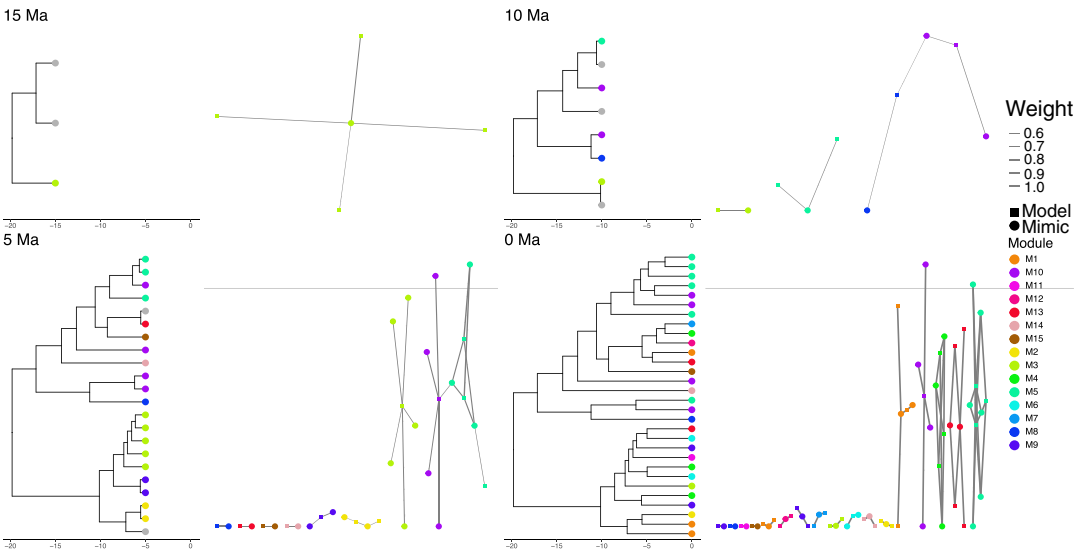

(legend on next page)

near the tip of the *D. cuellari* species group. ASTRAL analyses showed similar support values (local posterior probability [LPP] and normalized quartet support [NQS]) (see Figures S2 and S3). Conflicts between the trees occurred in regions with short internode distances and low NQS values, likely due to incomplete lineage sorting. Therefore, we proceeded with ASTRAL results for further phylogenetic comparisons as they accommodate incomplete lineage sorting.[8] The host phylogeny of *Pachyrhynchus* is from Van Dam et al.[9]

Divergence dating and biogeography of *Doliops* reveal limited dispersal with one back colonization of Luzon

Our independent rates analyses in MCMCTREE yielded a mean age of 19.8 Ma (95% HPD 16.1–23.7 Ma) for the *Doliops* root node. Most *Doliops* species diversified in the late Miocene and Pliocene epochs, with a mean node age of 7.1 Ma (95% HPD 5.1–9.4 Ma). The median node values for the *Doliops* clade were slightly lower at 6.0 Ma (median of nodes 95% HPD 4.1–8.1 Ma). While the mean node values did not overlap with the Pleistocene ($\leq$2.58 Ma), there are 8 nodes whose 95% lower bound overlaps, suggesting that most of the speciation events predated the glaciation cycles of the Pleistocene.

The results of BioGeoBEARS (Figure 4) analyses found that the best-fitting model, according to Akaike information criterion corrected for sample size (AICc) values, was the dispersal-extinction-cladogenesis + jump dispersal (DEC + J) model. The ancestral range reconstructions recover the *Doliops* root as occupying both Luzon and Mindanao islands of the Pleistocene aggregate island complex (PAIC). Despite the ability of *Doliops* to fly, there were relatively few independent colonization events. One of the main clades was reconstructed as originating in Luzon, and a second re-colonized Luzon from Panay. Mindoro had two independent colonization events, one from Mindanao and another from Luzon. The island of Panay was colonized from Mindanao. Only one separate back colonization of Mindanao occurred after the initial Luzon/Mindanao split. Most importantly, the lack of a reticulate biogeographic pattern indicates limited dispersal between islands.

Evaluation of cophylogenetic signal and the influence of biogeographic constraints

There were two main types of analyses that we conducted for evaluating model-mimic cophylogenetic signal and assessing the influence of biogeographic constraints: (1) we used the parafit method[10] to evaluate whether the speciation of the model species (*Pachyrhynchus*) had any effect on the speciation of the mimic (*Doliops*) and (2) we used an explicit model of host repertoire evolution to reconstruct the ancestral associations between the model (*Pachyrhynchus* species) and the mimics (*Doliops* species). This second analysis also allowed us to examine whether phylogenetic distance affected the ability of hosts to gain new parasites (in this case, mimetic species).[7] Because the *Pachyrhynchus-Doliops* mimetic system occurs on an island archipelago, we wanted to see whether the larger islands followed the same pattern as the entire system. If the global phylogenetic pattern supports cospeciation, but cospeciation is not supported within the individual islands, then biogeographic dispersal restrictions may be partially or entirely masking the within-island cospeciation signal.

Both methods (parafit and model of host repertoire evolution) supported a significant association between the host (model) and parasite (mimic). The parafit method had a p value of 0.001. In the model of host repertoire evolution, the "beta" parameter[11,12] identifies whether the phylogenetic distance between the host and parasite affects the ability of the host to gain a new parasite. To assess whether the fit of the parameter is significant, we tested whether our estimate significantly overlaps with 0. If the beta parameter is equal to 0, then gaining a new host/parasite from anywhere in the tree would be equally likely. The Bayes factor (BF) for the beta parameter significantly differed from zero, with a value of 2.7e + 18. Next, to examine the effect of biogeographic constraints, we tested for evidence of cospeciation within species occurring only on Luzon. Here, the two estimates of significance disagreed: the parafit method had a p value of 0.180 and the estimate of significance for the beta parameter was 5.8e + 9. This disagreement may be partly due to how the model of host repertoire evolution can distinguish between primary and secondary potential hosts, whereas in the parafit method, all associations are coded as equal. However, the Luzon clade's BF was substantially less than the global estimate.

Last, we examined the extent of coevolution in the Mindanao clade, as the other islands had too few species of *Doliops* ($N < 3$) to produce a robust result. The parafit method had a p value of 0.377 and the BF for the beta parameter was 1.11. Here, the two different estimates were more or less in agreement, with a BF $\sim$1 not considered to be strong support for one model being a better fit than another.[13,14] Again, as in the Luzon clade, both estimates indicate substantially less evidence for coevolution than global phylogenetic estimates. This suggests that at least some of the signals for coevolution in the global phylogenetic estimate are partly due to the clades' nested biogeographic nature (both host and parasites diversified within each island).

Doliops employ opal-like PCs of varying order in their color patterning

As in *Pachyrhynchus* weevils, *Doliops* longhorn beetles display various coloration patterns and colors on their elytra. These colors are created by assemblies of colorful scales that adorn their elytra (see Figures 3A and 3B). Using optical (light microscopy) and ultrastructural characterization techniques (small angle X-ray scattering [SAXS] and scanning electron microscopy [SEM]), we determined that the colors of these scales originate

Figure 2. Ancestral state reconstruction of host repertoire and interaction networks through time

Top, ancestral state reconstruction of host repertoire. Boxes at nodes indicate the ancestral state of host repertoire for which there was a >50% posterior probability for a particular host/parasite module. Bottom, *Doliops* and *Pachyrhynchus* interaction networks through three time slices and present network structure. In each time slice, the *Doliops* phylogeny is represented on the left and the interaction network is on the right. Circles represent *Doliops* species and squares represent *Pachyrhynchus* species. Color corresponds to the *Pachyrhynchus-Doliops* module. Line thickness of interaction networks corresponds to the posterior probability of the interaction. See also Figures S1–S4 for tree support values.

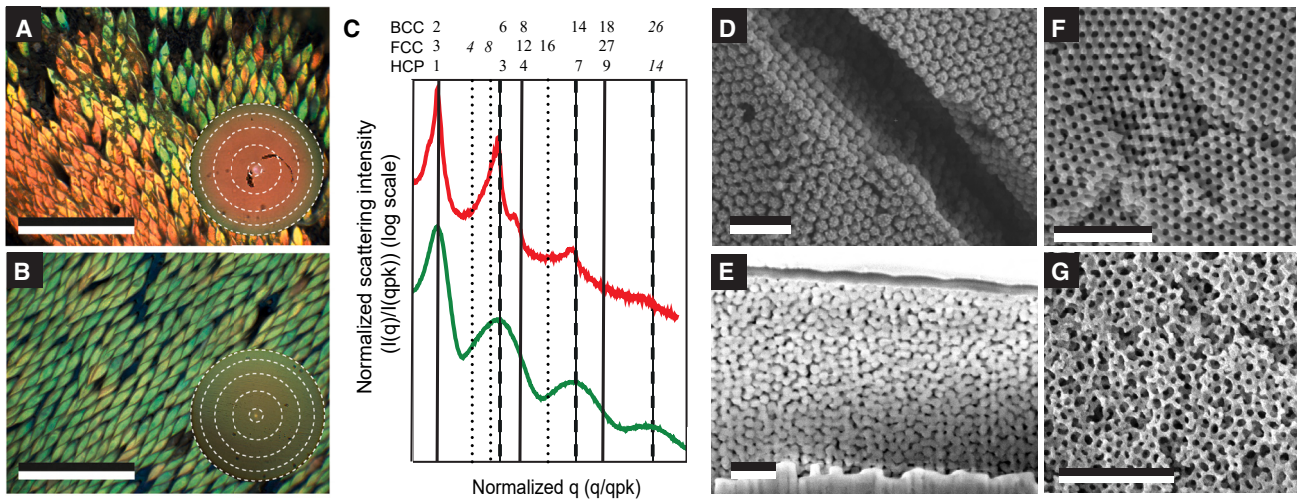

Figure 3. Photonic structure of *Doliops* scales

(A and B) Microscope images of (A) *D. metallicus* and (B) *D. cuellari*. Scale bars, 250 μm. (A and B) Inset: wide angle k-space images of the scales. White dotted rings in k-space images correspond to reflection angles of 5°, 20°, 35°, 50°, and 65°, respectively.

(C) Azimuthally averaged SAXS patterns of the scales from *D. metallicus* (red) and *D. cuellari* (green). The "q" factors and intensities are normalized to the first-order peak. The vertical lines correspond to the expected Bragg peak positions of the HCP space group (dashed lines) ($P6_3/mmc$), FCC (dotted lines), and BCC stackings (thin lines). Reflections common in all three space groups are shown with large black lines.

(D) SEM image of a scale in dorsal view from a *D. metallicus* specimen.

(E) Cross-sectional image of a *D. cuellari* scale.

(F) *P. congestus mirabilis* SEM image of an ordered scale showing nanostructure; scale bar, 2.5 μm.

(G) *P. congestus mirabilis* SEM image of a quasi-ordered scale showing nanostructure; scale bar, 2.5 μm. See also Figure S5 for azimuthally averaged SAXS patterns of additional species and Table S2 for a list of structural characteristics of the ordered *Doliops* specimens.

from photonic structures within them. These ultrastructural studies reveal that the structures within the *Doliops*' scales are composed of chitin spherules arranged in two predominant structures: ordered or quasi-ordered. The size of these spheres ranges from 200 to 300 nm, depending on the color of the scales. These structures differ from those found in *Pachyrhynchus* weevils, which are predominantly based on a diamond network structure with varying amounts of disorder.[15]

The ordered chitin sphere structure originates from periodically assembled chitin sphere layers (Figures 3A and 3D). The SAXS analysis (Figure 3C) determined that these ordered structures possess a hexagonal close-packed (HCP) arrangement, as found in other beetle species.[15–17] Note that in some ordered specimens, e.g., *D. pachyrrhynchoides*, a mixture of both face-centered cubic (FCC) and HCP arrangements are found, with the crystalline arrangement of the spheres assembled into smaller, ordered domains. More direct tomographic investigations will be needed to unambiguously determine the ordered arrangement in all ordered scales, yet little influence on the optical response is expected.[17] In the case of these polycrystalline specimens, the SAXS scattering peaks are broadened. Typically, the ordered structures produce a bright and more saturated color than their quasi-ordered counterparts and possess a distinct iridescence, as shown via our k-space images (Figure 3A, inset).

In the case of the quasi-ordered scales, the sphere assemblies can also produce structural colors, although devoid of clear crystalline structures (Figure 3E). These structures are found in the majority of the *Doliops* species (21 of 32) (Figure 3B). The color originates from a sphere-like assembly that, when viewed via SEM, demonstrates a seemingly random arrangement of spheres with no visibly ordered domains. Typically, such spherical assemblies are referred to as random close-packed (RCP) due to the apparent lack of order in their arrangement. The SAXS scattering structure of *D. cuellari* closely resembles that of previously reported RCP structures[16,18] (Figure 3C). Various quasi-ordered structures analyzed in this study demonstrate variations within this scattering pattern (Figure S5), with variations in the broadness and number of the scattering peaks. These variations in the structure are also mirrored in the optical properties of the specimen, i.e., their reflected brightness and color saturation.

PC-scale-type ancestral state reconstructions indicate the conservation of scale types

To understand how changeable the PC scale types are in *Doliops* and to determine whether *Pachyrhynchus* exhibits a mirrored pattern, we reconstructed the ancestral scale types for *Doliops* and used the authors' previous analyses and data for *Pachyrhynchus*.[15] The PC ancestral state reconstructions in the *Doliops* tree should provide insights into whether they use the same levels of PC order with their analogous scale structures.

We selected the best-fitting model of discrete character evolution, given our observed PC states and phylogeny. The results of model selection found the symmetric transition rates (SYM) model to be the best fit for our data given the AIC weights. We found a total of 4 transitions from quasi-ordered to ordered PC, with only 1 transition from ordered to quasi-ordered. There was a single transition from ordered to having both quasi-ordered and ordered PCs. The outgroup taxa all had quasi-ordered PCs. Compared with *Pachyrhynchus*, with only 7/62 species

CellPress
OPEN ACCESS

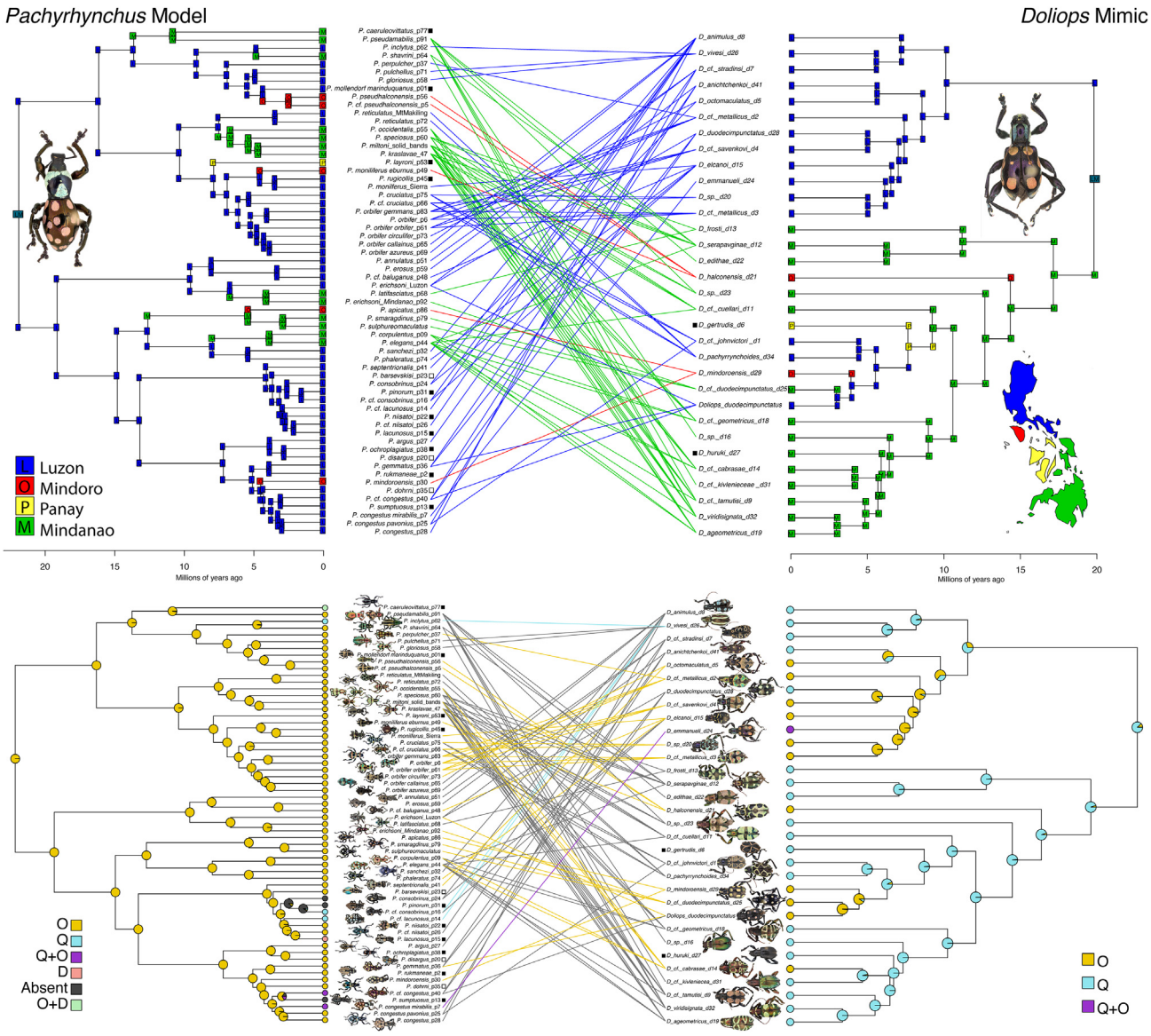

Figure 4. Ancestral state reconstructions for area and scale nanostructure

Lines in the center column link mimetic species. Top, BioGeoBEARS ancestral area reconstruction for *Pachyrhynchus* (left) *and Doliops* (right), both reconstructions used the best-fitting DEC + J model. The color of the lines corresponds to the species pairs' biogeographic area. Bottom, ancestral state reconstructions of scales' nanostructure. Letter codes correspond to a scale's photonic crystal state: (O) ordered, (Q) quasi-ordered, (D) disordered, and combinations thereof. The lines in the center are colored only if a mimetic pair shares the same photonic crystal type, e.g., both *Pachyrhynchus* and *Doliops* have ordered photonic crystals. Gray lines indicate that a mimetic pair has different types of photonic crystals. Filled squares near tips indicate species where a model or mimic is unknown; open squares indicate where a model or mimic is known but not sampled as the specimen was unavailable. See also Figures S1–S4 for tree support values.

containing quasi-ordered PCs, *Doliops* has 21/32 species with quasi-ordered PC. However, with only 4 transitions away from quasi-ordered to ordered PCs, most of the 11 species with ordered PCs occur in only 2 clades, indicating that the trait is conserved. When compared with *Pachyrhynchus*, most *Doliops* species do not have the same PC type, with only 10 completely matching. This indicates that PC type in *Pachyrhynchus* has little effect on PC type in *Doliops*. However, there is one instance where both ordered and quasi-ordered PC types occur in the same individual. In this species pair, the scale types are segregated on the pronotum (quasi-ordered) and elytra (ordered) (Figure 4; see also Table S2 for a list of structural characteristics of the ordered *Doliops* specimens).

DISCUSSION

Our first objective examined the extent to which coevolutionary interactions (in the form of mimetic assemblages) are conserved. If conserved, then we would expect to find cospeciation to be high and for the color patterns to be constrained for extended

periods of time. Here, we found that although a few interactions are conserved for long periods, as seen in the ancestral state reconstructions of the mimicry modules (Figure 2), many mimetic assemblages are transient and polyphyletic, likely influenced by local species assemblage. Our second objective examined whether codiversification patterns are driven primarily by biotic or abiotic factors. Our analyses indicate that abiotic factors (biogeography) are responsible for the global pattern of cospeciation between our Batesian mimetic pairs—the *Pachyrhynchus* weevil model and *Doliops* mimic. Lastly, we find that even at a nanoscale, mimicry produces novel structures in the emergence of ordered opal-like PCs within *Doliops*, so two independent evolutionary pathways are producing the same result from analogous structures.

We find that the within-island signal (Luzon and Mindanao) for cospeciation is either substantially less or absent, depending on what metric was used (parafit *p* value or BF). Within islands, both metrics indicate less cospeciation than the global pattern, indicating likely historical contingencies of colonization[19–21] rather than strict cospeciation as the predominant mode of mimicry development in *Doliops*. Importantly, local assemblages of weevils are phylogenetically diverse and often converge on the same pattern[9] and that often necessitates the *Doliops* longhorn beetles to mimic the local community assemblage rather than a single weevil species.[9]

There are some exceptions in which clades clearly reflect one another (Figure 1). For instance, the *P. orbifer* species groups and *D. magnificus* species groups have evolved an intricate color pattern that is not replicated by other species (Figures 2 and 4). Interestingly, while *Pachyrhynchus* species exhibit discrete color morphs (filled and open bands, see Figure 1, module M5 upper corner) in many species groups, *Doliops* species do not have the same type of discrete color polymorphisms. Our research shows that various *Doliops* species mimic a particular color morph of *Pachyrhynchus*, particularly the Mindanao species that mimics the *P. miltoni* species group (Figures 1 and 2), e.g., monophyletic *Pachyrhynchus* clade and polyphyletic assemblage of *Doliops*. In other instances where the local assemblage of *Pachyrhynchus* species have a close but not perfect resemblance (e.g., 2 cream-colored bands [*P. pseudamabilis*] instead of 3 [*P. miltoni*]), we also see variability in *Doliops* species (e.g., *D. tamutisi*) banding where the mimicry is imperfect. For instance, *Doliops* with three bands have varying distances between them, with some close together and some far apart. There are many species in this Mindanao mimicry complex, and geographic variation is rampant with intermediate forms—often described as separate species; precise geographic study of these populations could provide more clarity on how these color patterns emerge in both the models and mimics. Given the rarity of *Doliops*, they appear to follow the same syndrome of abundance (frequency model > frequency of mimic) as many other mimetic species where the host is not particularly harmful.[22]

To identify the presence of cospeciation, it is assumed that host/model switching is equally likely (independent) across the tree.[10] Thus, when the cophylogenetic distance between model and mimic species is shorter than it would be by chance, the cause is often interpreted as coevolution. Alternative processes generating cophylogenetic signals could include biogeographic barriers limiting the dispersal of hosts and parasites. In island settings where species ranges often do not overlap between islands and historical contingencies (founder events and priority effects) play a strong role in shaping communities, a pattern of cospeciation can be generated across the larger between-island phylogeny. In contrast, the local within-island pattern of cospeciation may be more stochastic. In continental settings, where biogeographic barriers may not be as discrete and where ranges overlap, biogeographic barriers may play much less of a role in shaping phylogenetic structure.[23] However, even in continental environments, habitat islands can shape the phylogenetic structure.[24] We examined a Batesian mimetic system on an island archipelago with discrete barriers to dispersal between islands, but they are differently porous to the model and the mimic because *Doliops* can fly. Therefore, it is essential to consider how biogeographic signals may influence the observed pattern of coevolution. Here, we found that the biogeographic history and pattern of cospeciation between models and mimics are linked. This linkage gives credence to the idea that biogeographic histories and historical contingencies of the colonization process play a role in the pattern of cospeciation within an island.

Additionally, we found that many individual interactions between species producing mimicry pairs may be short-lived (only found between a few tips rather than among entire clades). However, several patterns extend deeper into the tree and have existed for millions of years, as demonstrated by the results of our ancestral state and ancestral network reconstructions (Figures 1 and 2). For example, the widespread pattern of dots/spots, e.g., modules 4 and 6 (Figure 2). These longer-lasting interactions tend to occur in the more widespread and numerically abundant species based on collections, such as the *P. miltoni* group in Mindanao, indicating that whereas many closely related species may have slightly different variations on a theme, the general pattern exists for a longer time. Among the Luzon *Doliops*, the *D. metallicus* group produces ordered PCs, indicating that this change at the nanoscale may have been a key feature allowing for the persistence of mimicry between these two species complexes. However, there are other mimicry complexes in this clade that also have ordered PCs.

Lastly, compared with insect-host-plant interactions examined with similar methods, we found that mimicry patterns tend to be more modular, resulting in 17 independent ecological networks, indicating slightly more modularity. In contrast, Pieridae butterflies-angiosperm networks have 12 linked ecological networks, and these networks have a much longer duration, existing far longer than the *Doliops-Pachyrhynchus* networks, which typically last no more than ~5 million years on average.[7]

A more comprehensive framework for studying the coevolutionary dynamics between hosts and parasites is presented by considering historical contingencies, such as colonization events and biogeographic barriers. By doing so, we can more accurately discern the influence of biogeography on cospeciation, thereby shedding light on the actual processes underlying host-parasite coevolution. The *Doliops-Pachyrhynchus* system has limited evidence for specific clades tracking each other over long periods of time. Instead, the processes responsible for generating mimetic patterns more often involve lineage-independent interactions at the local community scale, as seen in the ancestral interaction networks and metrics of cospeciation. This suggests that chance historical contingencies of colonization are

the primary mode by which these two clades interact. How *Doliops* can be so labile in its host associations remains an open question. Possibly, the genetic basis of the PC's color and pattern, which remains unidentified, has enabled *Doliops* to adapt to the local *Pachyrhynchus* host assemblage.

RESOURCE AVAILABILITY

Lead contact

Further information and requests for resources and reagents should be directed to and will be fulfilled by the lead contact, Matthew H. Van Dam (mvandam@calacademy.org).

Materials availability

This study did not generate new unique reagents.

Data and code availability

The sequencing data have been deposited at NCBI and the accession number is provided in the key resources table. All data reported in this paper will be shared by the lead contact upon request.

Original code can be found in Data S1.

Any additional information required to reanalyze the data reported in this paper is available from the lead contact upon request.

ACKNOWLEDGMENTS

The authors would like to thank Dr. Mariana P. Braga for help with the *evolnets* and RevBayes module and discussion of methods and Prof. Ullrich Steiner for constant support. We would like to also thank Dr. Arvids Barsevskis (Daugavpils University, Latvia) and Dr. Eduard Vives (Natural Sciences Museum, Barcelona, Spain) for sharing images of some type specimens. The authors would like to thank the three anonymous reviewers and Dr. Sarah Crews (CAS) for their help in revising the paper. Funded in part through the National Science Foundation, Division of Environmental Biology award number 1856402 made to M.H.V.D. We thank Ruth Tawan-tawan, CEEO II of the Philippines' Department of Environment and Natural Resources Region XI, for help with the Gratuitous permits.

AUTHOR CONTRIBUTIONS

Conceptualization, M.H.V.D., A.W.L., A.A.C., M.N.M., A.P., and B.D.W.; data curation, M.H.V.D., A.P., and A.W.L.; formal analysis, M.H.V.D., N.G.-T., and A.P.; funding acquisition, M.H.V.D. and B.D.W.; methodology, M.H.V.D., B.D.W., A.A.C., and M.N.M.; project administration, M.H.V.D.; resources, M.H.V.D., A.W.L., A.A.C., M.N.M., and A.P.; software, M.H.V.D., N.G.-T., and A.P.; visualization, M.H.V.D. and A.P.; roles/writing – original draft, M.H.V.D. and A.W.L.; and writing – review & editing, M.H.V.D., A.W.L., A.A.C., M.N.M., A.P., and B.D.W.

DECLARATION OF INTERESTS

The authors declare no competing interests.

STAR★METHODS

Detailed methods are provided in the online version of this paper and include the following:

- KEY RESOURCES TABLE
- EXPERIMENTAL MODEL AND STUDY PARTICIPANT DETAILS
- METHOD DETAILS
  - DNA isolation and quality check
  - Library construction
- QUANTIFICATION AND STATISTICAL ANALYSIS
  - Low coverage genome assembly
  - Ultraconserved element (UCE) marker design
  - Extracting UCE loci and alignment construction
  - UCE phylogenomics
  - Concatenated phylogenetic analyses
  - Species tree analyses
  - Divergence dating biogeography
  - Evaluation of cophylogenetic signal
  - Photonic scale characterization
  - Photonic scale type ancestral state reconstructions

SUPPLEMENTAL INFORMATION

Supplemental information can be found online at https://doi.org/10.1016/j.cub.2024.09.084.

Received: May 30, 2024
Revised: August 6, 2024
Accepted: September 30, 2024
Published: October 22, 2024

REFERENCES

1. Mallet, J. (2010). Shift happens! Shifting balance and the evolution of diversity in warning colour and mimicry. Ecol. Entomol. *35*, 90–104. https://doi.org/10.1111/j.1365-2311.2009.01137.x.
2. Sherratt, T.N. (2008). The evolution of Müllerian mimicry. Naturwissenschaften *95*, 681–695. https://doi.org/10.1007/s00114-008-0403-y.
3. Mallet, J., and Joron, M. (1999). Evolution of Diversity in Warning Color and Mimicry: Polymorphisms, Shifting Balance, and Speciation. Annu. Rev. Ecol. Syst. *30*, 201–233.
4. Hembry, D.H., and Weber, M.G. (2020). Ecological Interactions and Macroevolution: A New Field with Old Roots. Annu. Rev. Ecol. Evol. Syst. *51*, 215–243. https://doi.org/10.1146/annurev-ecolsys-011720-121505.
5. Dismukes, W., Braga, M.P., Hembry, D.H., Heath, T.A., and Landis, M.J. (2022). Cophylogenetic Methods to Untangle the Evolutionary History of Ecological Interactions. Annu. Rev. Ecol. Evol. Syst. *53*, 275–298. https://doi.org/10.1146/annurev-ecolsys-102320-112823.
6. Hembry, D.H., Kawakita, A., Gurr, N.E., Schmaedick, M.A., Baldwin, B.G., and Gillespie, R.G. (2013). Non-congruent colonizations and diversification in a coevolving pollination mutualism on oceanic islands. Proc. Biol. Sci. *280*, 20130361. https://doi.org/10.1098/rspb.2013.0361.
7. Braga, M.P., Janz, N., Nylin, S., Ronquist, F., and Landis, M.J. (2021). Phylogenetic reconstruction of ancestral ecological networks through time for pierid butterflies and their host plants. Ecol. Lett. *24*, 2134–2145. https://doi.org/10.1111/ele.13842.
8. Sayyari, E., and Mirarab, S. (2016). Fast Coalescent-Based Computation of Local Branch Support from Quartet Frequencies. Mol. Biol. Evol. *33*, 1654–1668. https://doi.org/10.1093/molbev/msw079.
9. Van Dam, M.H., Anzano Cabras, A., and Lam, A.W. (2023). How the Easter Egg Weevils Got Their Spots: Phylogenomics Reveals Müllerian Mimicry in *Pachyrhynchus* (Coleoptera, Curculionidae). Syst. Biol. *72*, 516–529. https://doi.org/10.1093/sysbio/syac064.
10. Legendre, P., Desdevises, Y., and Bazin, E. (2002). A Statistical Test for Host–Parasite Coevolution. Syst. Biol. *51*, 217–234. https://doi.org/10.1080/10635150252899734.
11. Braga, M.P., van der Bijl, W., and Landis, M. (2023). evolnets: Reconstruct Ancestral Networks Inferred In RevBayes. R package version 0.0.0.9000.
12. Braga, M.P., Landis, M.J., Nylin, S., Janz, N., and Ronquist, F. (2020). Bayesian Inference of Ancestral Host-Parasite Interactions under a Phylogenetic Model of Host Repertoire Evolution. Syst. Biol. *69*, 1149–1162. https://doi.org/10.1093/sysbio/syaa019.
13. Jeffreys, H. (1961). Theory of Probability, Third Edition (Oxford University Press).

14. Huelsenbeck, J.P., Larget, B., and Alfaro, M.E. (2004). Bayesian Phylogenetic Model Selection Using Reversible Jump Markov Chain Monte Carlo. Mol. Biol. Evol. *21*, 1123–1133. https://doi.org/10.1093/molbev/msh123.

15. Parisotto, A., Steiner, U., Cabras, A.A., Van Dam, M.H., and Wilts, B.D. (2022). *Pachyrhynchus* Weevils Use 3D Photonic Crystals with Varying Degrees of Order to Create Diverse and Brilliant Displays. Small *18*, e2200592. https://doi.org/10.1002/smll.202200592.

16. Saranathan, V., Seago, A.E., Sandy, A., Narayanan, S., Mochrie, S.G.J., Dufresne, E.R., Cao, H., Osuji, C.O., and Prum, R.O. (2015). Structural Diversity of Arthropod Biophotonic Nanostructures Spans Amphiphilic Phase-Space. Nano Lett. *15*, 3735–3742. https://doi.org/10.1021/acs.nanolett.5b00201.

17. Parisotto, A., Saranathan, V., Steiner, U., and Wilts, B.D. (2023). Hexagonal-Close-Packed Colloidal Crystals in *Glenea celestis* Beetles. Small Sci. *3*, 2200114. https://doi.org/10.1002/smsc.202200114.

18. Djeghdi, K., Steiner, U., and Wilts, B.D. (2022). 3D Tomographic Analysis of the Order-Disorder Interplay in the *Pachyrhynchus congestus* mirabilis Weevil. Adv. Sci. (Weinh) *9*, e2202145. https://doi.org/10.1002/advs.202202145.

19. Gillespie, R.G. (2016). Island time and the interplay between ecology and evolution in species diversification. Evol. Appl. *9*, 53–73. https://doi.org/10.1111/eva.12302.

20. Gillespie, R. (2004). Community Assembly Through Adaptive Radiation in Hawaiian Spiders. Science *303*, 356–359. https://doi.org/10.1126/science.1091875.

21. Stroud, J.T., Delory, B.M., Barnes, E.M., Chase, J.M., De Meester, L., Dieskau, J., Grainger, T.N., Halliday, F.W., Kardol, P., Knight, T.M., et al. (2024). Priority effects transcend scales and disciplines in biology. Trends Ecol. Evol. *39*, 677–688. https://doi.org/10.1016/j.tree.2024.02.004.

22. Finkbeiner, S.D., Salazar, P.A., Nogales, S., Rush, C.E., Briscoe, A.D., Hill, R.I., Kronforst, M.R., Willmott, K.R., and Mullen, S.P. (2018). Frequency dependence shapes the adaptive landscape of imperfect Batesian mimicry. Proc. Biol. Sci. *285*, 20172786. https://doi.org/10.1098/rspb.2017.2786.

23. Wilson, J.S., Williams, K.A., Forister, M.L., von Dohlen, C.D., and Pitts, J.P. (2012). Repeated evolution in overlapping mimicry rings among North American velvet ants. Nat. Commun. *3*, 1272. https://doi.org/10.1038/ncomms2275.

24. Van Dam, M.H., and Matzke, N.J. (2016). Evaluating the influence of connectivity and distance on biogeographical patterns in the south-western deserts of North America. J. Biogeogr. *43*, 1514–1532. https://doi.org/10.1111/jbi.12727.

25. McKenna, D.D., Scully, E.D., Pauchet, Y., Hoover, K., Kirsch, R., Geib, S.M., Mitchell, R.F., Waterhouse, R.M., Ahn, S.-J., Arsala, D., et al. (2016). Genome of the Asian longhorned beetle (Anoplophora glabripennis), a globally significant invasive species, reveals key functional and evolutionary innovations at the beetle–plant interface. Genome Biol. *17*, 227. https://doi.org/10.1186/s13059-016-1088-8.

26. Chen, S., Zhou, Y., Chen, Y., and Gu, J. (2018). fastp: an ultra-fast all-in-one FASTQ preprocessor. Bioinformatics *34*, i884–i890. https://doi.org/10.1093/bioinformatics/bty560.

27. R Core Team (2021). R: A Language and Environment for Statistical Computing (R Foundation for Statistical Computing). https://www.R-project.org/.

28. Bankevich, A., Nurk, S., Antipov, D., Gurevich, A.A., Dvorkin, M., Kulikov, A.S., Lesin, V.M., Nikolenko, S.I., Pham, S., Prjibelski, A.D., et al. (2012). SPAdes: A New Genome Assembly Algorithm and Its Applications to Single-Cell Sequencing. J. Comput. Biol. *19*, 455–477. https://doi.org/10.1089/cmb.2012.0021.

29. Manni, M., Berkeley, M.R., Seppey, M., Simão, F.A., and Zdobnov, E.M. (2021). BUSCO Update: Novel and Streamlined Workflows along with Broader and Deeper Phylogenetic Coverage for Scoring of Eukaryotic, Prokaryotic, and Viral Genomes. Mol. Biol. Evol. *38*, 4647–4654. https://doi.org/10.1093/molbev/msab199.

30. Faircloth, B.C., McCormack, J.E., Crawford, N.G., Harvey, M.G., Brumfield, R.T., and Glenn, T.C. (2012). Ultraconserved Elements Anchor Thousands of Genetic Markers Spanning Multiple Evolutionary Timescales. Syst. Biol. *61*, 717–726. https://doi.org/10.1093/sysbio/sys004.

31. Heibl, C. (2008). PHYLOCH: R language tree plotting tools and interfaces to diverse phylogenetic software packages. http://www.christophheibl.de/Rpackages.html.

32. Katoh, K., Misawa, K., Kuma, K., and Miyata, T. (2002). MAFFT: a novel method for rapid multiple sequence alignment based on fast Fourier transform. Nucleic Acids Res. *30*, 3059–3066. https://doi.org/10.1093/nar/gkf436.

33. Capella-Gutiérrez, S., Silla-Martínez, J.M., and Gabaldón, T. (2009). trimAl: a tool for automated alignment trimming in large-scale phylogenetic analyses. Bioinformatics *25*, 1972–1973. https://doi.org/10.1093/bioinformatics/btp348.

34. Kozlov, A.M., Darriba, D., Flouri, T., Morel, B., and Stamatakis, A. (2019). RAxML-NG: a fast, scalable and user-friendly tool for maximum likelihood phylogenetic inference. Bioinformatics *35*, 4453–4455. https://doi.org/10.1093/bioinformatics/btz305.

35. Yin, J., Zhang, C., and Mirarab, S. (2019). ASTRAL-MP: scaling ASTRAL to very large datasets using randomization and parallelization. Bioinformatics *35*, 3961–3969. https://doi.org/10.1093/bioinformatics/btz211.

36. Zhang, C., Rabiee, M., Sayyari, E., and Mirarab, S. (2018). ASTRAL-III: polynomial time species tree reconstruction from partially resolved gene trees. BMC Bioinformatics *19* (*Suppl 6*), 153. https://doi.org/10.1186/s12859-018-2129-y.

37. Mai, U., and Mirarab, S. (2018). TreeShrink: fast and accurate detection of outlier long branches in collections of phylogenetic trees. BMC Genomics *19* (*Suppl 5*), 272. https://doi.org/10.1186/s12864-018-4620-2.

38. Junier, T., and Zdobnov, E.M. (2010). The Newick utilities: high-throughput phylogenetic tree processing in the U_{nix} shell. Bioinformatics *26*, 1669–1670. https://doi.org/10.1093/bioinformatics/btq243.

39. Yang, Z. (2007). PAML 4: Phylogenetic Analysis by Maximum Likelihood. Mol. Biol. Evol. *24*, 1586–1591. https://doi.org/10.1093/molbev/msm088.

40. Puttick, M.N. (2019). MCMCtreeR: functions to prepare MCMCtree analyses and visualize posterior ages on trees. Bioinformatics *35*, 5321–5322. https://doi.org/10.1093/bioinformatics/btz554.

41. Dos Reis, M., and Yang, Z. (2013). The unbearable uncertainty of Bayesian divergence time estimation. J. Syst. Evol. *51*, 30–43. https://doi.org/10.1111/j.1759-6831.2012.00236.x.

42. Matzke, N.J. (2014). Model Selection in Historical Biogeography Reveals that Founder-Event Speciation Is a Crucial Process in Island Clades. Syst. Biol. *63*, 951–970. https://doi.org/10.1093/sysbio/syu056.

43. Paradis, E., Claude, J., and Strimmer, K. (2004). APE: Analyses of Phylogenetics and Evolution in R language. Bioinformatics *20*, 289–290. https://doi.org/10.1093/bioinformatics/btg412.

44. Sztucki, M. (2021). SAXSutilities2: a graphical user interface for processing and analysis of Small-Angle X-ray Scattering data. Zenodo. https://doi.org/10.5281/zenodo.5825707.

45. Revell, L.J. (2012). phytools: an R package for phylogenetic comparative biology (and other things). Methods Ecol. Evol. *3*, 217–223. https://doi.org/10.1111/j.2041-210X.2011.00169.x.

46. Faircloth, B.C. (2017). Identifying conserved genomic elements and designing universal bait sets to enrich them. Methods Ecol Evol *8*, 1103–1112. https://doi.org/10.1111/2041-210X.12754.

47. Van Dam, M.H., Henderson, J.B., Esposito, L., and Trautwein, M. (2021). Genomic Characterization and Curation of UCEs Improves Species Tree Reconstruction. Syst. Biol. *70*, 307–321. https://doi.org/10.1093/sysbio/syaa063.

48. Mirarab, S. (2019). Species Tree Estimation Using ASTRAL: Practical Considerations. Preprint at arXiv. https://doi.org/10.48550/arXiv.1904.03826.

49. Hall, R. (2002). Cenozoic geological and plate tectonic evolution of SE Asia and the SW Pacific: computer-based reconstructions, model and animations. J. Asian Earth Sci. *20*, 353–431. https://doi.org/10.1016/S1367-9120(01)00069-4.

50. Ashman, L.G., Shin, S., Zwick, A., Ślipiński, A., and McKenna, D.D. (2022). The first phylogeny of Australasian Lamiinae longhorn beetles (Coleoptera: Cerambycidae) reveals poor tribal classification and a complex biogeographic history. Syst. Entomol. *47*, 213–230. https://doi.org/10.1111/syen.12526.

51. Zhu, T., Dos Reis, M., and Yang, Z. (2015). Characterization of the Uncertainty of Divergence Time Estimation under Relaxed Molecular Clock Models Using Multiple Loci. Syst. Biol. *64*, 267–280. https://doi.org/10.1093/sysbio/syu109.

52. Dos Reis, M., and Yang, Z. (2011). Approximate Likelihood Calculation on a Phylogeny for Bayesian Estimation of Divergence Times. Mol. Biol. Evol. *28*, 2161–2172. https://doi.org/10.1093/molbev/msr045.

53. Inger, R.F. (1954). Systematics and zoogeography of Philippine Amphibia. In Fieldiana, *33* (Chicago Natural History Museum), pp. 182–531.

54. Heaney, L.R. (1986). Biogeography of mammals in SE Asia: estimates of rates of colonization, extinction and speciation. Biol. J. Linn. Soc. *28*, 127–165. https://doi.org/10.1111/j.1095-8312.1986.tb01752.x.

55. Brown, R.M., and Siler, C.D. (2014). Spotted stream frog diversification at the Australasian faunal zone interface, mainland versus island comparisons, and a test of the Philippine 'dual-umbilicus' hypothesis. J. Biogeogr. *41*, 182–195. https://doi.org/10.1111/jbi.12192.

56. Ree, R.H., and Smith, S.A. (2008). Maximum Likelihood Inference of Geographic Range Evolution by Dispersal, Local Extinction, and Cladogenesis. Syst. Biol. *57*, 4–14. https://doi.org/10.1080/10635150701883881.

57. Ronquist, F. (1997). Dispersal-Vicariance Analysis: A New Approach to the Quantification of Historical Biogeography. Syst. Biol. *46*, 195–203. https://doi.org/10.1093/sysbio/46.1.195.

58. Landis, M.J., Matzke, N.J., Moore, B.R., and Huelsenbeck, J.P. (2013). Bayesian Analysis of Biogeography when the Number of Areas is Large. Syst. Biol. *62*, 789–804. https://doi.org/10.1093/sysbio/syt040.

59. Brown, R.M., Su, Y.-C., Barger, B., Siler, C.D., Sanguila, M.B., Diesmos, A.C., and Blackburn, D.C. (2016). Phylogeny of the island archipelago frog genus Sanguirana: Another endemic Philippine radiation that diversified 'Out-of-Palawan'. Mol. Phylogenet. Evol. *94*, 531–536. https://doi.org/10.1016/j.ympev.2015.10.010.

60. Conow, C., Fielder, D., Ovadia, Y., and Libeskind-Hadas, R. (2010). Jane: a new tool for the cophylogeny reconstruction problem. Algorithms Mol. Biol. *5*, 16. https://doi.org/10.1186/1748-7188-5-16.

61. Balbuena, J.A., Pérez-Escobar, Ó.A., Llopis-Belenguer, C., and Blasco-Costa, I. (2020). Random Tanglegram Partitions (Random TaPas): An Alexandrian Approach to the Cophylogenetic Gordian Knot. Syst. Biol. *69*, 1212–1230. https://doi.org/10.1093/sysbio/syaa033.

62. Höhna, S., Landis, M.J., Heath, T.A., Boussau, B., Lartillot, N., Moore, B.R., Huelsenbeck, J.P., and Ronquist, F. (2016). RevBayes: Bayesian Phylogenetic Inference Using Graphical Models and an Interactive Model-Specification Language. Syst. Biol. *65*, 726–736. https://doi.org/10.1093/sysbio/syw021.

63. Schnablegger, H., and Singh, Y. (2017). The SAXS Guide: Getting Acquainted with The Principles (Anton Paar GmbH).

STAR★METHODS

KEY RESOURCES TABLE

REAGENT or RESOURCE	SOURCE	IDENTIFIER
Deposited data		
Raw and analyzed data	This paper	NCBI-SRA: PRJNA1118243
Anoplophora glabripennis genome assembly	McKenna et al.[25]	NCBI: GCF_000390285.2
Software and algorithms		
fastp version-0.20.0	Chen et al.[26]	https://github.com/OpenGene/fastp
R v4.2.2	R Core Team[27]	https://www.r-project.org/
SPAdes-3.11.1	Bankevich et al.[28]	https://github.com/ablab/spades?tab=readme-ov-file
BUSCO v5.4.5	Manni et al.[29]	https://gitlab.com/ezlab/busco/-/releases#5.4.0
PHYLUCE	Faircloth et al.[30]	https://phyluce.readthedocs.io/en/latest/
ips	Heibl[31]	https://github.com/heibl/ips
R scripts	Van Dam et al.[9]	https://academic.oup.com/sysbio/article/72/3/516/6702792
R scripts	Current study, Data S1	–
MAFFT	Katoh et al.[32]	https://mafft.cbrc.jp/alignment/software/
trimAl	Capella-Gutiérrez et al.[33]	https://github.com/inab/trimal
RAxML-NG	Kozlov et al.[34]	https://github.com/amkozlov/raxml-ng
ASTRAL-MP	Yin et al.[35]	https://github.com/smirarab/ASTRAL
ASTRAL-III	Zhang et al.[36]	https://github.com/smirarab/ASTRAL
TreeShrink	Mai and Mirarab[37]	https://github.com/uym2/TreeShrink
Newick_utilities	Junier and Zdobnov[38]	https://github.com/tjunier/newick_utils
PAML 4	Yang[39]	https://abacus.gene.ucl.ac.uk/software/
MCMCtreeR	Puttick et al.[40]	https://github.com/PuttickMacroevolution/MCMCtreeR
baseml	Dos Reis and Yang[41]	https://abacus.gene.ucl.ac.uk/software/
BioGeoBEARS v1.1.2	Matzke[42]	https://github.com/nmatzke/BioGeoBEARS
Ape	Paradis et al.[43]	https://cran.r-project.org/web/packages/ape/index.html
Evolnets	Braga et al.[11]	https://github.com/maribraga/evolnets
SAXSutilities2	Sztucki[44]	https://www.saxsutilities.eu/
Phytools	Revell[45]	https://github.com/liamrevell/phytools

EXPERIMENTAL MODEL AND STUDY PARTICIPANT DETAILS

We used pinned museum specimens from the Davao Oriental State University Biodiversity Collection, Mindanao, Philippines for this study, and voucher specimens are also deposited here.

METHOD DETAILS

DNA isolation and quality check

The specimens were dissected carefully to exclude the beetle's abdomen to minimize contaminants, using legs and tissue from the pronotum. In some specimens, contaminants were apparent upon examination (e.g., fungus and mites), and in those cases, legs were removed and punctured to allow enzymatic (proteinase-K) digestion of soft tissue, procedures largely followed those of Van Dam et al.[9] DNA was extracted from the resulting digest using the QIAamp micro kit (Qiagen, Germany) following the manufacturer's protocol. We assessed the quantity of all isolated DNA using a Qubit 2.0 Fluorometer (Invitrogen, USA). DNA quality (i.e., fragment size distributions) was determined using 1% agarose gel or, for historic samples with low starting concentrations, a 2100 BioAnalyzer (Agilent Technologies, USA). Our starting DNA quality and quantity varied significantly among specimens: from 4.8 ng–5000 ng and 200 bp–50 kbp.

Library construction

We obtained paired-end Illumina data from 43 whole genome libraries. When necessary, DNA was sheared using a Covaris M220 (Covaris Inc., USA). Libraries were constructed with the NEBNext® Ultra™II DNA Library Preparation kit

(New England Biolabs Inc, USA) following the manufacturer's protocol. To minimize PCR replicates in the final dataset, we titrated the number of PCR cycles as described in Van Dam et al.[9] The average sizes of the final libraries were around 250 bp to 400 bp.

QUANTIFICATION AND STATISTICAL ANALYSIS

Low coverage genome assembly

First, we trimmed any remaining adapters and low-quality bases from the ends of our reads with *fastp* version-0.20.0 using the "detect_adapter_for_pe" setting.[26] We then combined unpaired reads into a single file for each species. Next, we used *SPAdes-3.11.1*[28] to assemble the reads into scaffolds with k-mer values of 21, 33, 55, 77, 99 and 127 in the *SPAdes* assembly pipeline using default settings for everything other than the memory ("-m 800") and cpu threads ("-t 32"). We then ran BUSCO v5.4.5[29] with the Insecta lineage data set (isnecta_odb10) on our assemblies to assess their completeness. See Table S1 for assembly results.

Ultraconserved element (UCE) marker design

We designed a custom ultraconserved element (UCE) probe set using the PHYLUCE pipeline[30] (Faircloth[46]). To maximize the effectiveness of the probes, we selected individuals that spanned the morphological diversity of our taxa. For the base taxon, we used the Cerambycidae species *Anoplophora glabripennis* genome assembly.[25] This taxon was used as the initial bait set because: 1) The genome is complete, 2) The genome is free of contamination, which can lead to off-target loci capture,[9] 3) The genome is soft masked for repetitive elements. We only selected loci that were recovered in our base taxon. Additionally, at the time of our UCE loci development (2020), there were no chromosome-scale and/or more completely annotated genomes available. This genome was particularly well-suited because it was also in the same subfamily as our target taxon (Laminae). Additionally, we could eliminate loci from off-target species (contaminants), because it was so thoroughly annotated and screened. In total, we included 6 species (5 *Doliops* sp. and *A. glabripennis*) in our probe design, including the base taxon, see Table S1. We only kept loci that were shared between all six species in our bait design.

Because our phylogenetic scope was limited in our probe design and no annotated *Doliops* genome exists, we were conservative in our probe design, keeping only those probes found in the base genome plus the other 5 taxa. We found a total of 39,278 loci in our initial design. After annotating the loci to the *A. glabripennis* genome annotation (General Feature Format file (gff)), we identified 11,444 loci as exon-only, 11,535 loci as intron-only, 730 loci as exon-and-intron (spanning exon-intron boundaries), and 15,569 loci as intergenic.

Extracting UCE loci and alignment construction

We largely followed the PHYLUCE pipeline[30] to match, extract, and align our probe set. Other settings follow Van Dam et al.[9] Unless otherwise noted, we used the default settings. We used the PHYLUCE script "phyluce_probe_run_multiple_lastzs_sqlite" with an "identity" of 60. After matching probes to scaffolds, we used "phyluce_probe_slice_sequence_from_genomes" to extract the flanking 500 bases around our probes. After the initial alignment step using *mafft*,[32] we used "phyluce_align_get_trimal_trimmed_alignments_from_untrimmed" to internally trim our matrices. This step uses *trimAl*[33] to help trim ambiguously aligned sites in the alignments. We used "phyluce_align_get_only_loci_with_min_taxa" to select loci with a minimum of 80% complete matrices. Lastly, we used "phyluce_align_format_nexus_files_for_raxm" to produce the final concatenated matrix.

UCE phylogenomics

We used two types of analyses for phylogenetic reconstruction: (1) a concatenated analysis using RAxML-NG v1.0.0,[34] and (2) a summary species tree analysis using ASTRAL-MP v5.7.4.[35,36]

Concatenated phylogenetic analyses

We used the General Time Reversible + gamma (GTRGAMMA) site rate substitution model across our alignment with 10 independent parsimony-based starting trees for our maximum-likelihood (ML) searches in RAxML-NG. Non-parametric bootstrap replicates (BS) were done using the autoMRE option, with a maximum of 200 replicates to optimize the number of bootstrap replicates for this large dataset. Lastly, we mapped the bootstrap replicate values onto the best-scoring ML tree.

Species tree analyses

Identifying cogenic-UCE loci

We used methodologies that are similar to Van Dam et al.[47] for combining UCE loci that were cogenic. We then used the R[27] package *ips*[31] with an *R* script from Van Dam et al.[47] We removed any columns composed exclusively of "-","n" and/or "?" using the "deleteEmptyCells" function, followed by removing any ragged ends of the matrix with the "*trimEnds*" function, with a minimum of 4 taxa present in the alignment. Using scripts from Van Dam et al.[47] we identified the basic genomic characteristics of our UCEs and concatenated cogenic UCEs as in Van Dam et al.[47] We provide an updated code from Van Dam et al.[47] for easier use in combining cogenic UCEs (see Data S1).

Gene tree and species tree reconstruction

We used 10 independent parsimony-based starting trees for our maximum likelihood (ML) searches in RAxML-NG. We looked for outlier branches using TreeShrink[37] with option -b 50 because lower values tended to remove outgroups given our tree shape.

We re-ran the analysis with outliers removed. We then performed 100 non-parametric bootstrap replicates and mapped the bootstrap replicate values onto the best-scoring ML tree. Next, we collapsed/contracted branches in the gene trees with BS $\leq$20 using newickutils[38]; this has been demonstrated to have a strong positive impact on the accuracy of species tree reconstruction.[48] The resulting trees were used in species tree reconstruction. We used ASTRAL-MP with the default settings to reconstruct the species tree and annotate the tree with support values calculated for the normalized quartet support (NQS) and local posterior probability (LPP).[8]

Divergence dating biogeography

We used MCMCTREE[39] to perform our divergence dating analyses with the topology from our ASTRAL analyses as the starting topology. No fossils exist for the ingroup or near relatives, so we used a geological calibration for the maximum age of the Philippine Islands, 25–30 Ma as the root node between *Doliops* and *Stenodoliops* because they are both endemic to the Philippines. This is an approximate date for the emergence of the Philippine proto-islands proposed by Hall.[49] We set the maximum age for our clade based on the estimates of Ashman et al.[50] for the divergence between *A. glabripennis* and *Callimetopus gloriosus*, a near relative of *Acronia* (>62.5<108 Ma). We used MCMCtreeR[40] to format our calibration point on the tree file for MCMCTREE. Next, we used the tree to obtain an estimate of the substitution rate using basml[41] by selecting single UCE loci with >90% complete matrices, resulting in 294 loci. Using more loci may prevent the analysis from completing, and using more data is unnecessary to approximate the uncertainty of the divergence dates.[51,52] Finally, we estimated the gradient and Hessian of the branch lengths[52] in the final estimation of our divergence dates.

To reconstruct the broad-scale biogeographical patterns of *Doliops*, we used BioGeoBEARS v1.1.2.[42] Because biogeographic model selection is sensitive to duplicate taxa, we removed all potential duplicates from the same metapopulation lineage/species.[42] We defined our areas according to the Pleistocene Aggregate Island Complex (PAIC) hypothesis.[53–55] We examined 3 different biogeographic models, (DEC[56]; DIVA-like[57]; BAYAREA-like[58]) and also included the "+J" parameter for founder-event/jump speciation at cladogenesis events.[42] This parameter has been demonstrated to greatly improve model fit for island and island-like systems.[24,42,59] We used the Akaike information criterion corrected for sample size (AICc) to identify which model best explained our data given the number of free parameters.

Evaluation of cophylogenetic signal

We used several different metrics to evaluate cophylogenetic signal. For example, one method for reconstructing cophylogenetic relationships optimizes the cost of events (cospeciation, duplication, duplication and host switch, and loss).[60] However, the event cost methods assumes that the cospeciation event has no cost, which may not always be true.[5] A second method uses a global fit between the host and parasite.[10,61] These global fit methods examine if there is a correlation between the host and parasite phylogenies using the principal coordinates from phylogenetic distance matrices. We used the *parafit* method in the R package ape to assess the global fit of our trees.[10,43] Next, we used a method that implements a model of host-parasite coevolution,[12] implemented in RevBayes[62] v1.2.4 and the *evolnets*[11] R package. This alternative to distance measures not only identifies if there is an effect of evolutionary distance between host and parasite but, more significantly, uses an explicit model to reconstruct the ancestral associations between the host and parasites. Here, we used the estimates of the 'beta' parameter,[7] which determines whether the phylogenetic distance between the host and parasite affects the probability of gaining a new host.[7] This method also allows one to assign probabilities to the ancestral states.

To reconstruct the ancestral ecological networks between *Doliops* and *Pachyrhynchus*, we used the *evolnets* package,[7,11] which assigns taxa to modules based on their interaction probabilities derived from an ancestral host repertoire reconstruction analysis.[5] This results in modules comprised by taxa that interact more frequently with each other than with other taxa and quantifies interaction patterns, aiding in the characterization of ecological networks.[7]

To examine the effect that biogeography may have on influencing cophylogenetic pattern, we analyzed species from the two largest Philippine Islands (Luzon and Mindanao) separately. The smaller islands have fewer than 4 species of *Doliops*, so the analyses for the smaller islands were not conducted. For the two single islands analyses, we pruned the main tree to retain only species that reside on these islands. Then, we conducted the parafit and 'beta' parameter Bayes Factor tests of cophylogenetic signal within each island as described above.

Photonic scale characterization

The ultrastructural properties of the *Doliops* specimens were determined with a scanning electron microscope (SEM), a focused ion beam coupled to an SEM (FIB-SEM) as well as the use of small angle x-ray scattering (SAXS).

To analyze *Doliops'* scale ultrastructure via SEM, these were first removed from the specimen with the use of a needle and then placed onto conductive carbon tape. The scales were then opened via a plasma etching procedure and were exposed to a 4:20 oxygen to argon plasma for 12–15 minutes. This treatment was performed with the use of a PE-100 RIE Benchtop Plasma Etching System (Plasma Etch Inc., Carson City, NV, USA). After the plasma etching, the scales were coated with 4–8 nm of gold or platinum (Cressington Scientific Instruments, Watford, England). The dorsal view micrographs of the specimen's scales were made using either a Tescan Mira3 LM FE SEM (Tescan, Brno, Czechia) or a ThermoFisher Scios 2 DualBeam FIB-SEM (FEI, Eindhoven, the Netherlands). To take lateral view or cross-sectional images, the scales were milled with a ThermoFisher Scios 2 FIB. To perform the FIB milling process, it was first necessary to use a gas injection system (GIS) to deposit approximately 1 micron of platinum

onto the scales to avoid deformation of the sample during the milling process. After the platinum deposition, a trench was milled in front of the cross-section to be imaged to allow the specimen to be imaged from an angle. The majority of the trench was milled at a voltage of 30 kV with a current of 1 nA. Progressively finer currents ranging from 0.1–0.01 nA were then used to prepare the final cross-section for imaging. Once the trench was dug, the specimen was imaged with an SEM. The SEM imaging was performed at an angle of 52 degrees, so a tilt correction was applied to remove image distortions.

SAXS scattering was performed at the IDO2 beamline of the European Synchrotron Radiation Facility in Grenoble. Here, the scales from various *Doliops* specimens were scraped onto 0.003 mm thick kapton adhesive and sandwiched with another piece of kapton tape. Background measurements were taken through bare kapton adhesive. The samples were placed directly into the pinhole SAXS detector where measurements were performed in transmission with a pinhole size of approximately 15 microns horizontal and 15 microns vertical. To process the SAXS plots and convert them into azimuthal averages (i.e., intensity/q plots), SAXS utility software was used.[44] Once these plots were prepared, their peaks were indexed and compared to previously reported biological structures[16] and other SAXS index databases.[63]

Photonic scale type ancestral state reconstructions

We first coded each species' scale type accordingly. Next, we selected the best-fitting model of discrete character evolution given our observed PC states and phylogeny. We examined 3 different models of discrete character evolution using the *phytools* function fitMK (''SYM'', ''ER'' and ''ARD'' models)[45] both as ordered and unordered transitions. We then calculated the best-fitting model for our data using the AIC weights. Next, using the best-fitting model, we reconstructed the ancestral states onto our chronogram analyses (using same tree used in BioGeoBEARS) with the *phytools* function make simmap with 20,000 stochastic mappings. We used the results from Parisotto et al.[15] for *Pachyrhynchus*' ancestral state reconstructions using identical methods.